

Paper to be presented at the 1998 International Conference on Simulation Technology for Nuclear Power Plants and Systems, January 11-16, 1998, San Diego, California.

ANL/RE/CP--94525
CONF-980120-

Parallelization of the MAAP-A Code Neutronics/Thermal
Hydraulics Coupling

P. H. Froehle, T. Y. C. Wei and D. P. Weber
Reactor Engineering Division
Argonne National Laboratory
9700 South Cass Avenue
Argonne, IL 60439

and

R. E. Henry
Fauske & Associates, Inc.
16W070 West Eighty-third Street
Burr Ridge, IL 60521

The submitted manuscript has been authored by a contractor of the U. S. Government under contract No. W-31-109-ENG-38. Accordingly, the U. S. Government retains a nonexclusive, royalty-free license to publish or reproduce the published form of this contribution, or allow others to do so, for U. S. Government purposes.

MASTER

DISTRIBUTION OF THIS DOCUMENT IS UNLIMITED 

¹ Work supported by the U.S. Department of Energy, Energy Research Programs under Contract W-31-09-ENG-38.

DISCLAIMER

This report was prepared as an account of work sponsored by an agency of the United States Government. Neither the United States Government nor any agency thereof, nor any of their employees, makes any warranty, express or implied, or assumes any legal liability or responsibility for the accuracy, completeness, or usefulness of any information, apparatus, product, or process disclosed, or represents that its use would not infringe privately owned rights. Reference herein to any specific commercial product, process, or service by trade name, trademark, manufacturer, or otherwise does not necessarily constitute or imply its endorsement, recommendation, or favoring by the United States Government or any agency thereof. The views and opinions of authors expressed herein do not necessarily state or reflect those of the United States Government or any agency thereof.

DISCLAIMER

**Portions of this document may be illegible
in electronic image products. Images are
produced from the best available original
document.**

CONF-980120--

PARALLELIZATION OF THE MAAP-A CODE NEUTRONICS/THERMAL HYDRAULICS COUPLING

P. H. Froehle, T. Y. C. Wei, D. P. Weber and R. E. Henry*
Reactor Engineering Division
Argonne National Laboratory
9700 South Cass Avenue
Argonne, IL 60439

Nuclear Engineering

Computer Software

Multiprocessors

ABSTRACT

A major new feature, one-dimensional space-time kinetics, has been added to a developmental version of the MAAP code through the introduction of the DIF3D-K module. This code is referred to as MAAP-A. To reduce the overall job time required, a capability has been provided to run the MAAP-A code in parallel. The parallel version of MAAP-A utilizes two machines running in parallel, with the DIF3D-K module executing on one machine and the rest of the MAAP-A code executing on the other machine. Timing results obtained during the development of the capability indicate that reductions in time of 30% - 40% are possible. The parallel version can be run on two SPARC 20 (SUN OS 5.5) workstations connected through the ethernet. MPI (Message Passing Interface standard) needs to be implemented on the machines. If necessary the parallel version can also be run on only one machine. The results obtained running in this one-machine mode identically match the results obtained from the serial version of the code.

1.0 INTRODUCTION

A major new capability, one-dimensional space-time kinetics, has been added to a developmental version of the MAAP code through the coupling of the DIF3D-K module to MAAP (Henry, Paik and Plys 1994). This code has been designated as MAAP-A. With the introduction of this major new modelling capability in the one dimensional space-time kinetics it became apparent through the results of timing studies that the computation time of the MAAP-A code would be affected when the new DIF3D-K space-time neutronics module (Taiwo 1992) was used. Parallel computing, that is running different parts of the code on different machines, in parallel, is an option which could reduce this effect on the total job time. Since job time would have to be spent on passing data between the different machines for the computation to proceed, optimization of the code decomposition between the different machines and the number of machines selected would be required. Minimal data passing and maximal computation effort between data passing would

be ideal for reducing the total job time and increasing the efficiency of the parallelization scheme. In addition for maximum utilization of each of the machines involved to achieve maximum parallelization efficiency, the computing load among the different machines should be equally balanced. A number of alternatives were considered for decomposing the code between different machines running in parallel. Timing and dataflow studies performed on the code using a spectrum of typical reactor plant transients concluded that the best computing performance would be obtained by the functional decomposition scheme where the DIF3D-K module (neutronics function) was run on one machine and the MAAP module (thermal-hydraulics function) was run in parallel on a second machine. These results were obtained for SPARC 20 work stations connected through the ethernet. MPI (Message Passing Interface standard) (Snir, Otto, Huss-Lederman, Walker and Dongarra 1996) was used as the system required to provide the data (or message) passing capability between the different machines executing in parallel. MPI version 1.0.13 July 26, 1996 was used during the development phase of the code. The parallel version of MAAP-A therefore executes on two workstations (with MPI) running in parallel with the DIF3D-K module on one machine and the MAAP (rest of MAAP-A) module on the other machine. This decomposition of the MAAP-A code leads to a degree of decoupling between the neutronics simulation on one machine and the thermal-hydraulics (T-H) simulation on the other machine during the time period when no data exchange takes place. A number of decoupling schemes are possible. The one selected for implementation is the One Step Lag scheme (OSL) where the neutronics computation lags the T-H computation by one time step. Section 2.0 provides the general theory which forms the conceptual basis for the parallelization scheme. Section 3.0 provides test case results from the MAAP-A parallel code structure which implemented this parallelization scheme.

2.0 GENERAL THEORY

Phenomena (functional) decomposition is the parallelization strategy where the simulation of different physical

phenomena proceed in parallel on separate machines. For MAAP/DIF3D-K the two major phenomena involved are neutronics and thermal-hydraulics. When the two coupled phenomena are calculated in parallel on separate machines a certain amount of decoupling between the phenomena occurs during the time when no data interchange is taking place. This affects the overall accuracy of the coupled simulation. Decoupling choices made to effect the parallelization affect the accuracy of the simulation. It is difficult to analyze these effects with the complete set of one dimensional space-time neutronics equations of DIF3D-K and the complete set of MAAP-A T-H equations. We illustrate these effects with a simplified set of model equations based on point kinetics and a lumped thermal energy equation. Since we are only interested in the implications for the transient coupling between the two phenomena and are not particularly concerned about spatial dependencies for the parallelization on two processors, we restrict our discussion to one independent variable, time. There are a number of dependent variables. Since the spatial dependence is not of interest, the total core fission power (P) will be the focus for the neutronics phenomena. It is also the neutronics variable which couples to the T-H. It is assumed for the purposes of this illustration that the coupling to the neutronics of the T-H is through the enthalpy/temperature (T) and only through enthalpy/temperature so T will be the only dependent T-H variable referred to here. The model equations for this coupling between neutronics and T-H are then

$$\frac{dP}{dt} = \gamma TP + \delta_o P + N_o \quad (1)$$

$$\frac{dT}{dt} = -\frac{T}{\tau} - \eta P + \frac{T_a}{\tau} \quad (2)$$

with

$$\rho = \rho_o + \alpha(T - T_o) \quad (3)$$

where

$$\gamma = \frac{\alpha}{\ell} \quad \delta_o = \frac{\rho_o - \alpha T_o - \beta}{\ell} \quad \lambda C_o = N_o$$

$$\tau = Mc/hA \quad \eta = (Mc)^{-1}$$

- λ = decay constant
- C = precursor concentration
- M = mass
- c = specific heat
- ℓ = neutron lifetime

- β = delayed neutron fraction
- ρ = reactivity
- α = reactivity coefficient
- h = heat transfer coefficient

subscript

- o = steady state value
- a = ambient

Equation (1) can be recognized to be the core fission power equation of the one delay group point kinetics set of equations. Since the precursor concentration plays a minor role in the neutronics-T/H coupling we set it to be constant at the steady state value. Equation (2) is a lumped thermal inertia energy equation for the core where heat losses are homogenized into the heat transfer coefficient term. Equation (3) is the equation for reactivity where the only dependence is on core temperature. Temperature is the only T-H variable which affects reactivity and thereby core fission power in this model problem. This is all that is necessary to establish a mathematical coupling from the T-H to the neutronics in this presentation. Physically the coupling is through the temperature dependence of the cross sections $\Sigma(T)$ which is approximated by the use of the term $\alpha(T - T_o)$ in the reactivity equation. The mathematical and physical coupling from the neutronics to the T-H is through the P term in Eq. (2).

We first give a qualitative analysis of possible decoupling schemes and the implications for parallelization or more correctly, the sequencing of the solutions of the two equations. After the qualitative analysis, a more formal mathematical analysis is presented with the consequent implications for solution accuracy. The formal mathematical analysis will examine the finite difference equations. The notation will be changed slightly with \tilde{P}_k used instead of P_k in the finite difference equations. First order finite differencing of the time derivatives in Eqs. (1) and (2) will be used. Depending upon the degree of implicitness used the right hand side of Eqs. (1) and (2) can have several different forms. For this analysis we treat all the non-coupled terms on the RHS as explicit. The degree of implicitness of the coupling terms $\{(\gamma TP)$ in Eq. (1) and ηP in Eq. (2)] will be varied. It is understood that MAAP, as coded, treats the non-coupled terms on the RHS of Eq. (2) as explicit. It is also understood that DIF3D-K, as coded, varies the degree of implicitness of the non-coupled terms on the RHS of Eq. (1) depending upon user option selected. This should not affect the analyses presented here as it focuses on the implications of the treatment of the coupling terms. The degree of decoupling determines the degree of implicitness of the coupling terms which in turn determines the accuracy of the solution scheme. For this work we have examined the following four decoupling schemes: (A) Discretized Reality, (B) Sequential/Serial Scheme, (C) One Step Lag Scheme,

(D) Virtual Step Lag Scheme. In this paper we discuss schemes (A) and (C).

(A) Discretized Reality: This is the analysis of what actually happens physically and what the ideal parallel computation scheme should be, taking into account the discrete time step. Reference should be made to Fig. 1. Figure 1 shows the real time axes for the neutronics (DIF3D-K) computation and the T-H (MAAP) computation respectively. The dashed vertical lines show the time synchronization between the two processors relative to the real time. The figure will be referred to as a time diagram. The bottom time line shows the temperature T_k at time t_k . The top time line shows the corresponding power P_k at time t_k . At each t_k the temperature $T_k(P_{k-1}, P_k)$ is determined as a function of both beginning and end of time step powers, P_{k-1} and P_k as should be expected physically. It is the history of the power over the time interval $\Delta t_{k-1, k}$ which determines the end of time step temperature T_k . Since we are discretizing in time the functionality $T_k(P_{k-1}, P_k)$ should be a reasonable approximation. Similarly the power $P_k(\Sigma(T_{k-1}), \Sigma(T_k))$ shows the functionality where the cross sections $\Sigma(T_{k-1})$ and $\Sigma(T_k)$ determine the end of time step power. This should reasonably approximate the cross-section time history effect on the power during the interval $\Delta t_{k-1, k}$. These temperature and power functionalities should be a reasonable approximation of the phenomena coupling over the time step and should be utilized for the ideal computation scheme. This degree of coupling demanded of the two simultaneous calculations is not possible since end of time step values are not available at the beginning of the time step. Short of several iterations between the two computations for each time step, additional approximations have to be made. Intuitively one would think that Discretized Reality would use the following finite difference equations,

$$\frac{\bar{P}_{k-1} - \bar{P}_k}{\Delta t} = \gamma \frac{(T_{k-1} + T_k)}{2} \bar{P}_k + \delta_0 \bar{P}_k - N_0 \quad (4)$$

$$\frac{T_{k+1} - T_k}{\Delta t} = -\frac{T_k}{\tau_{k,k-1}} + \eta_{k,k-1} \frac{(\bar{P}_{k+1} + \bar{P}_k)}{2} + \frac{T_a}{\tau_{k,k-1}} \quad (5)$$

where the coupling terms are treated semi-implicitly. Equations (4) and (5) of course adhere to the convention, stated earlier, of explicit treatment of the non-coupling terms. These equations serve as the idealized reference for the decoupling scheme to be discussed.

(C) One Step Lag Scheme: To be able to perform the two computations simultaneously the concept of a lag in the functionalities is needed. Variations on the lag concept can be implemented. One would like to improve the accuracy but be able to retain the feature of parallel computation between the neutronics and the T-H. Figure 2 shows the time diagram for the One Step Lag (OSL) scheme. Comparison with Fig. 1 shows that there is an actual one step lag in the computation of the power behind the T-H. The synchronization of the two processors has a one step lag in it. A start is made with T_1 calculated using P_0 . But the neutronics calculation is not started until the first T-H step is completed. The T-H condition at t_1 , T_1 is passed to the neutronics calculation to form $\Sigma(T_1)$ at t_1 . The power change is then calculated over the interval Δt_{01} using Σ_0 and $\Sigma(T_1)$ to arrive at the functionality $P_1(\Sigma_0, \Sigma(T_1))$. While this computation is being performed the T-H computation is proceeding a step ahead over the interval from t_1 to t_2 using P_0 to arrive at $T_2(P_0)$. At this point the power P_1 at t_1 is known from the neutronics computation. P_1 is then used over the next interval t_2 to t_3 to give the functionality $T_3(P_1)$. The T-H conditions at t_2 , T_2 are passed to the neutronics computation and used to form $\Sigma(T_2)$ at t_2 . This is then utilized in the neutronics computation, which is lagging by one processor step, to calculate the power change over the interval t_1 to t_2 . This gives the functionality at t_2 of $P_2(\Sigma(T_1), \Sigma(T_2))$ and establishes the pattern for the P and T sequence as time proceeds. We now have $P_k(\Sigma(T_{k-1}), \Sigma(T_k))$. As can also be seen by comparing with Fig. 1, Discretized Reality is no better.

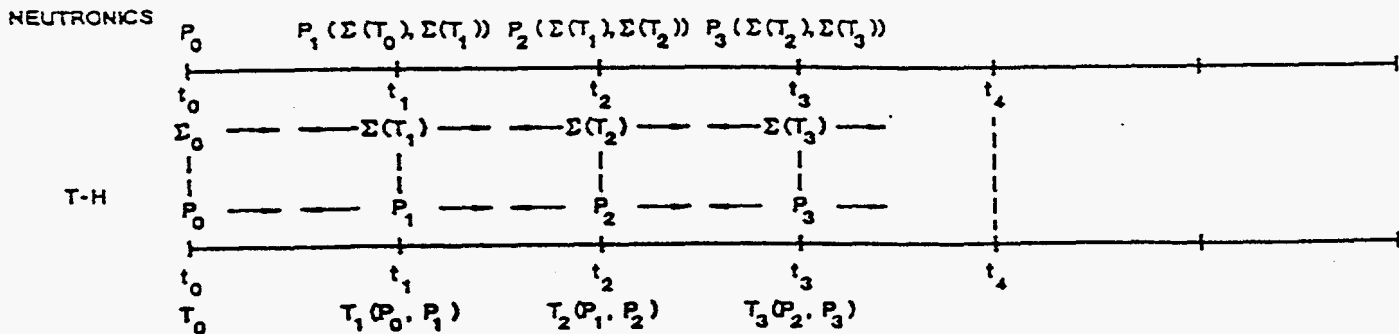


Fig. 1. Discretized Reality Scheme Time Diagram.

It should be noted though that this improvement in the power results cannot be expected to improve the temperature results since the neutronics calculation of the power is always one processor step behind. For T-H driven accident initiators this should be relatively more acceptable. For reactivity driven accident initiators the reverse lag would be more acceptable. The change which will enable parallelization to occur is to modify the power coupling in Eq. (5) to \bar{P}_{k-1} which is an explicit treatment with an additional time delay. The equations are now

$$\frac{\bar{P}_{k+1} - \bar{P}_k}{\Delta t} = \gamma \frac{(T_k + T_{k-1})}{2} \bar{P}_k + \delta_o \bar{P}_k - N_o \quad (6)$$

$$\frac{T_{k+1} - T_k}{\Delta t} = -\frac{T_k}{\tau_{k,k+1}} + \eta_{k,k-1} \bar{P}_{k-1} + \frac{T_a}{\tau_{k,k-1}} \quad (7)$$

It can be shown that the time diagram for the semi-implicit temperature/explicit power delay treatment corresponds to the one presented in Fig. 2. The One Step Lag Scheme uses finite difference equations with a semi-implicit temperature/explicit power delay treatment.

One could perform a consistency and convergence-in-the-limit analysis to determine the relative accuracy of the various finite difference forms to explore the relative accuracy of the different schemes. However, by qualitatively comparing the sets of equations with Discretized Reality (which should be the most accurate form) a qualitative ranking could be extracted. Based on this we could expect the accuracy ranking to be, Discretized Reality - Sequential/Serial Scheme - One Step Lag Scheme - Virtual Step Lag Scheme. The One Step Lag (OSL) scheme has been selected for the code decomposition scheme. The numerical accuracy of the parallel code using the OSL scheme can be anticipated to be less than that of the serial code. However developmental results

obtained for a number of thermal-hydraulically driven transients show that acceptable comparisons can be obtained.

The advantage of the OSL scheme over the other code decomposition schemes investigated is that the thermal-hydraulic step size is known before the neutronic calculation is performed at any given time. There will therefore be no need to back up in simulation time for either the neutronics or thermal-hydraulic calculations as there will be no overshoot between the two calculations. This leads to more efficient utilization of machine computation time and therefore should result in larger reductions in total job time.

3.0 TESTING RESULTS

A number of test calculations for a matrix of transients have been performed to verify the parallelization performance of the code. Calculations have been performed for both MAAP-A BWR (BMAAP-A) and MAAP-A PWR (PMAAP-A). The MAAP-A BWR cases have focused on a typical BWR plant while those for MAAP-A PWR have focused on a typical PWR plant. Table 1 shows the matrix of transients.

Results are presented for an assessment of both the code numerical performance and for the code timing performance. Numerical comparison of variables for accuracy and timing statistics are provided. Code numerical performance is discussed first and then code timing performance is detailed.

In order to assess the numerical performance of MAAP-A BWR, the core power and key core T-H quantities, important to the space-time neutronics, calculated with the parallel version of MAAP-A were compared with those calculated by the serial version. Key T-H quantities considered were the primary system pressure, two-phase void fraction in the core, core average coolant density, and average fuel temperature in the core. The calculations were performed for an integrated plant transient. The specific transient which was selected was

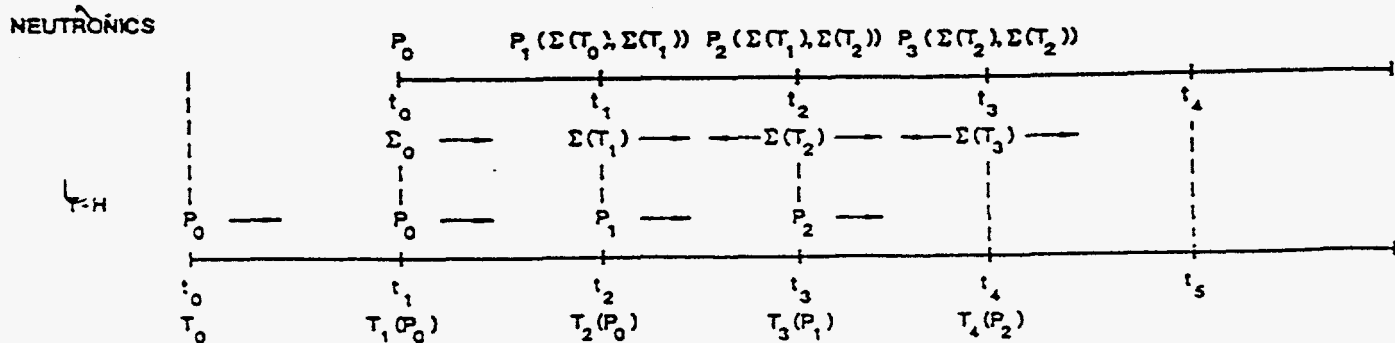


Fig. 2. One Step Lag Scheme Time Diagram.

Table 1. Matrix of Test Cases

Test Code	Plant	Test Case
MAAP-A BWR	B-Plant (B-P)	MSIV closure without scram
		Small Break LOCA without scram
		Turbine trip test with delayed scram (TT w delay scram)
		Small Break LOCA without scram and additional trips
MAAP-A PWR	P-Plant (P-P)	Large Break LOCA with scram
		Main Steam Line Break with scram (MSLB)

the turbine trip transient at the B-Plant where the scram was intentionally delayed to provide confirmatory data. Figures 3 to 5 show the first 10 seconds of the B-Plant turbine trip with delayed scram test transient. In all figures the solid curve is the serial code version result while the dashed curve is the parallel code version result. The parallel version results are obtained by running the version on two processors. The total core power is shown in Fig. 3. This is the power used on the MAAP side of the parallel calculations and drives the MAAP phenomena. It is the sum of the fission power and the decay power averaged over the MAAP time step. Figure 3 shows good agreement in total core power calculated in the parallel and in the serial versions. This comparison is important because in MAAP-A the fission power calculation is done in the new module DIF3D-K using the one dimensional space-time kinetics. Figure 4 shows the decay power. Figure 5 shows the prediction of the primary system pressure after the closing of the turbine stop valve. The primary system pressure rises to pressurize the vessel and collapse the core voids. In both Figs. 4 and 5 there is essentially little difference between the serial results and the parallel results. Similarly for the remaining key T-H variables no difference is visible between the serial results and the parallel results. In summary these results show that the parallel version of MAAP-A BWR is calculating powers and thermal-hydraulic quantities key to the powers which are essentially the same as those produced by the serial version of MAAP-A BWR.

In order to assess the numerical performance of MAAP-A PWR a similar procedure was followed. The core power and key core T-H quantities, important to the space-time neutronics, calculated with the parallel version of MAAP-A were compared with those from the serial version. Key T-H quantities considered were the primary system pressure, mass

of subcooled water in the core, core average two phase void fraction, core average coolant density, and average fuel temperature in the core. Figures 6 to 8 show the first 600 seconds of the P-Plant Main Steam Line Break transient. In all figures the solid curve is the serial code version result while the dashed curve is the parallel code version result. The total core power is shown in Fig. 6. Figure 6 shows good agreement in total core power calculated in the parallel and in the serial versions. Figure 7 shows the decay power. Figure 8 shows prediction of the primary system pressure during the steam line break. The primary system pressure falls as the steam line break on the secondary side overcools the primary system. In both Figs. 7 and 8 there is essentially little difference between the serial results and the parallel results. Similarly for the remaining T-H variables no difference is visible between the serial results and the parallel results. In summary these results show that the parallel version of MAAP-A PWR is calculating powers and thermal-hydraulic quantities key to the powers which are essentially the same as those produced by the serial version of MAAP-A PWR.

The timing performance of the parallel version of MAAP-A is evaluated by obtaining timing statistics for the set of test problems. Table 2 presents the timing results from the serial code calculation and from the corresponding parallel code calculation for these test problems. The serial code calculation is performed on a dedicated single SPARC 20 station under SOLARIS 2.5. The parallel code calculation is performed on two dedicated processors; one of which is the SPARC 20 utilized for the serial calculation and the second of which is another SPARC 20 station with the same configuration. The two processors are connected through an Ethernet network. MPI version 1.3 is used for the message passing between the two parallel processors. The input files, parameter files and nuclear data files used are for each of the test problems listed in Table 1.

In the PROCESS column of Table 2 "ser" refers to the serial results, while "par2-0" refers to the results obtained for parallel processor 0 which is running the MAAP-A thermal hydraulic models. The row "par2-1" refers to the timing results obtained for the other work station, parallel processor 1, which runs the DIF3D-K space-time neutronics model. TOTALTIME is the sum of the CPUTIME and the SYSTEMTIME. This is ETIME on SOLARIS 2.5. CPUTIME is the time the job is using when it is not asking the operating system to perform a task. SYSTEMTIME is the time the operating system requires to run the job while WALLTIME is the wall clock time. ITSTEP is the total number of MAAP-A thermal hydraulic time steps. The last column PERF is the ratio of the WALLTIME for the maximum of the par2 processors to WALLTIME for the ser processor. This is in effect the percentage of the parallel calculation time relative

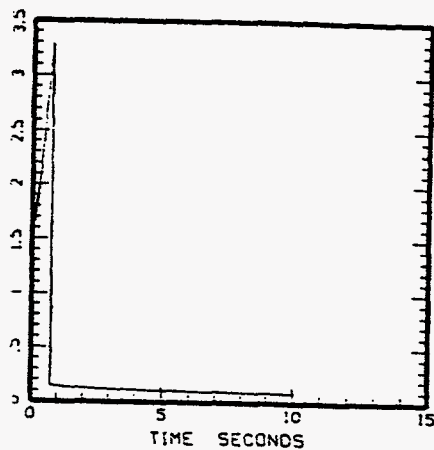


Fig. 3. B-P TT w dly scram
Total Core Power.

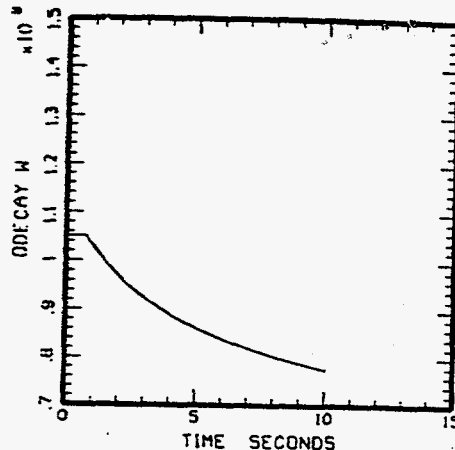


Fig. 4. B-P TT w dly scram
Decay Power.

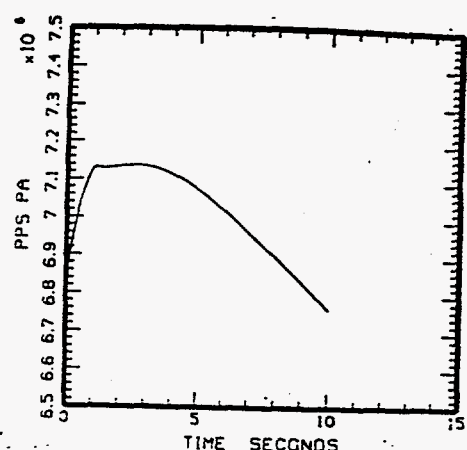


Fig. 5. B-P TT w dly scram
Primary Pressure.

Table 2. MAAP-A Code Timing Performance Results

TEST CODE	TEST CASE	PROCESS	TOTALTIME	WALLTIME	ITSTEP	PERF
MAAP-A BWR	MSVI closure without scram	ser	498.49	587.63	1889	60%
		par2-0	288.05	351.90	2212	
		par2-1	347.13	351.92	2212	
	Small Break LOCA without scram	ser	2076.26	2522.51	10113	59%
		par2-0	1442.04	1494.17	10063	
		par2-1	1476.52	1492.68	10063	
	Turbine trip test with delayed scram	ser	90.27	109.74	277	54%
		par2-0	47.91	59.12	293	
		par2-1	58.66	59.12	293	
	Small Break LOCA without scram and additional trips	ser	1243.71	1469.09	4700	56%
		par2-0	845.26	882.70	5467	
		par2-1	870.37	882.71	5467	
MAAP-A PWR	Large Break LOCA with scram	ser	4114.81	4578.62	14237	73%
		par2-0	2770.42	3368.38	13498	
		par2-1	2448.62	3369.95	13498	
	Main steam line break with scram	ser	245.65	288.21	784	56%
		par2-0	135.86	160.47	783	
		par2-1	159.55	160.47	783	

to the serial calculation time. For perfect load balance between the two processors and negligible message passing time, which is the ideal situation, the minimum PERF ratio would be 50%. This would be the optimum performance. For most of the MAAP-A cases shown in Table 2, PERF is in the range 55-60%. This is close to the optimum performance value of 50%. For one MAAP-A PWR case shown in Table 2 the value is closer to 75%. The reason for this is that in the Large Break

LOCA P-Plant test case, core degradation with hydrogen generation and eventual core melting with fuel relocation occurs. Core degradation starts to occur at ~7500 seconds. In MAAP-A the space-time neutronics model is turned off once these severe accident core degradation conditions start to occur. Once core degradation starts to occur, the validity of the one-dimensional neutronics assumption and the use of the intact geometry group cross sections start to degrade. Once the

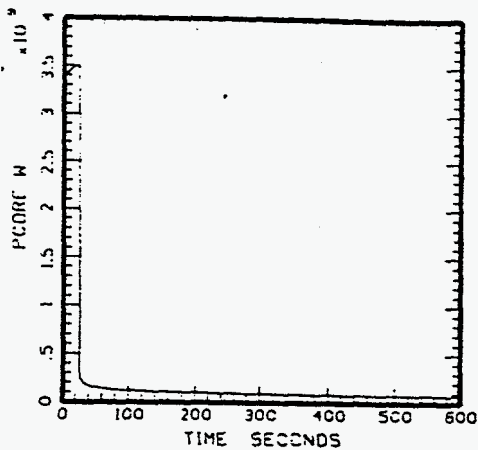


Fig. 6. P-P MSLB
Total Core Power.

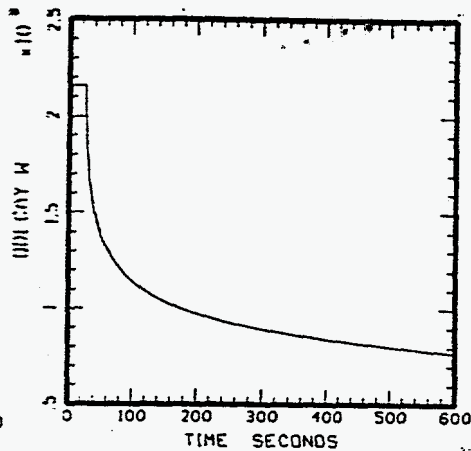


Fig. 7. P-P MSLB
Decay Power.

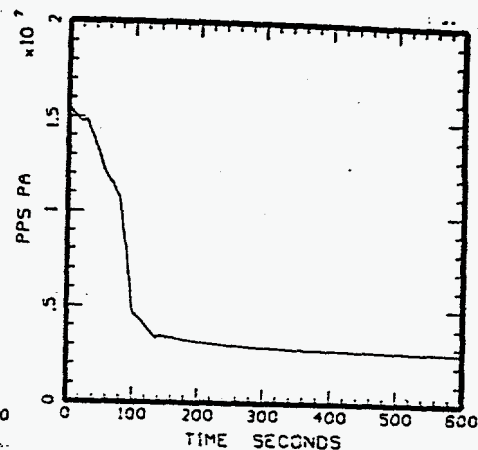


Fig. 8. P-P MSLB
Primary Pressure.

space-time neutronics model is bypassed the computational load becomes very unbalanced and the parallel performance starts to degrade. Since the calculation of the degraded core conditions is a significant part of the computation time, PERF is affected significantly. This explains the result presented in Table 2 for this MAAP-A PWR case. However, in general the results obtained and presented in Table 2 for the two test problems show that the parallel code performs well in terms of computation time. The conclusion to draw is that the parallelization algorithm which was implemented in the code functions as intended.

4.0 SUMMARY

A major new capability, one-dimensional space-time kinetics, has been added to a developmental version of the MAAP code through the introduction of the DIF3D-K module. Use of this space-time kinetics capability can affect the computation time of the new MAAP-A code. To reduce the overall job time required, a feature has been provided to run the MAAP-A code in parallel. The parallel version of MAAP-A utilizes two machines running in parallel, with the DIF3D-K module executing on one machine and the rest of the MAAP-A code executing on the other machine. Initialization of the code is performed on both machines at the beginning of the run. Timing results obtained during the development of the capability indicate that reductions in time of 30% - 40% are possible. The theoretical maximum is 50% if both machines are utilized at 100% efficiency. MAAP-A cases with the space-time neutronics model can therefore be executed in about the same computation time as MAAP 4 cases without the space-time neutronics model if the transient scenarios do not change. It should be noted that the efficiency is problem dependent. For those reactor plant transients where each thermal hydraulic time step requires only one neutronic time step, good efficiencies can be expected. The parallel

version can be run on two SPARC 20 (SUN OS 5.5) workstations connected through the ethernet. MPI (Message Passing Interface standard) needs to be implemented on the machines. MPI version 1.0.13 July 26, 1996 was used during the development phase of the code. If necessary the parallel version can also be run on only one machine. The results obtained running in this one-machine mode identically match the results obtained from the serial version of the code.

REFERENCES

- Henry, R.E., Paik, C.Y. and Plys, M.G. 1994. *MAAP4 - Modular Accident Analysis Program for LWR Power Plants*, Volume 1. FAI Report (May).
- Snir, M.S., Otto, S., Huss-Lederman, S., Walker, D. and Dongarra, J. 1996. *MPI: The Complete Reference*, The MIT Press, Cambridge, MA.
- Taiwo, T.A. 1992. *DIF3D-K: A Nodal Kinetics Code for Solving the Time-Dependent Diffusion Equation in Hexagonal-Z Geometry*, Argonne National Laboratory Report. ANL/NPR-92/17.

ACKNOWLEDGMENTS

We wish to thank R. Hammersley and B. Schlenger-Faber of FAI and J. A. Stillman of ANL for their valuable support. We also express our gratitude to Jason Chao of EPRI for his efforts and to EPRI for granting the permission to use MAAP. Acknowledgment is due to Judy Wozniak for her careful typing of this paper.

Work supported by the U.S. Department of Energy, Office of Energy Research Laboratory Technology Transfer Program under contract W-31-109-ENG-38.